International Journal of Chemical, Materials and Biomolecular Sciences
ISSN: 2415-6620
Vol:9, No:6, 2015

The Effect of Aging of ZnO, AZO, and GZO Films on the Microstructure and Photoelectric Property

Zue Chin Chang

***Abstract*—**RF magnetron sputtering is used on the ceramic targets, each of which contains zinc oxide (ZnO), zinc oxide doped with aluminum (AZO) and zinc oxide doped with gallium (GZO). The XRD analysis showed a preferred orientation along the (002) plane for ZnO, AZO, and GZO films. The AZO film had the best electrical properties; it had the lowest resistivity of 6.6×10^{-4} cm, the best sheet resistance of 2.2×10^{-1} Ω/square, and the highest carrier concentration of 4.3×10^{20} cm^{-3}, as compared to the ZnO and GZO films.

***Keywords*—**Aging, films, Microstructure, Photoelectric Property.

I. Introduction

IT is common to use transparent conducting oxides (TCOs), such as indium tin oxide (ITO), in optoelectronic devices such as solar cells and flat panel displays due to its low electrical resistivity (about ~10^{-4} Ω cm) and relatively high work function [1]. However, the cost of preparing ITO films is very high because indium is a rare and expensive element [2]. Transparent conducting zinc-oxide (ZnO), a II-VI n-type semiconductor with a wide band gap of approximately 3.3 eV at room temperature, has been widely used as a TCO material because it is low in cost, readily available, and non-toxic and has good chemical stability and high optical transmission [3]. Although ZnO is a potential candidate to replace ITO, its conductivity is lower than those of other metals. To eliminate that drawback, the introduction of metal dopants and/or metal-nanoparticles has been investigated [4].

Impurity-doped ZnO thin films such as Ga-doped zinc oxide (GZO) and Al-doped zinc oxide (AZO), having high transmittance and low resistivity, have attracted much attention as alternatives to ITO film. AZO and GZO films are advantageous because their primary components are inexpensive zinc oxide series films. These AZO and GZO films are known to demonstrate increased conductivity due to the oxygen defects of ZnO, which is their primary component, and the increased use of AZO and GZO films can be realized if the conductivity and optical transparency can be raised to levels close to those of ITO film. Although both AZO and GZO are promising TCO candidate materials, GZO still has three main advantages over AZO for several reasons. First, Ga has a higher resistance to oxidation during deposition than Al. Second, the diffusivity of Ga is relatively low compared to that of Al, so fewer diffusion-related problems (e.g., contamination) occur in the final products. Finally, less lattice distortion and fewer lattice defects are generated in GZO than in AZO, even at high concentrations of Ga, because the Ga-O bond length (0.192 nm) is close to that of Zn-O (0.197 nm) [5], [6].

Currently, TCO films can be prepared by RF magnetron sputtering, metal organic chemical vapor deposition (MOCVD), pulsed laser deposition (PLD), molecular beam epitaxy (MBE), and Sol-Gel methods. Among them, RF magnetron sputtering can be performed at lower temperatures with better quality, and it is widely used in industry and academia [7]-[12]. Some researchers think that the electrical properties of AZO and GZO thin films can be improved with the use of different annealing conditions [13]-[16], but almost no reports have examined the influence of chemical etching on the electrical properties of these films. Therefore, in the present study, ZnO, GZO, and AZO thin films were deposited by RF magnetron sputtering and then annealed and chemically etched by NaOH solution. The surface morphologies, crystal structures, and electrical and optical properties of the thin films were also investigated.

ZnO, AZO, and GZO thin films with thicknesses of 200 nm and 400 nm were deposited on glass by RF magnetron sputtering using 4-inch-diameter targets of ZnO, AZO (ZnO : Al_2O_3 =98:2 wt. %, and GZO (ZnO:Ga_2O_3 = 95:5 wt. %). The base pressure of the deposition chamber was kept at 2.5×10^{-6} torr and the working pressure at 2.5×10^{-3} torr by a rotation-type mechanical pump and a turbo pump, and the sputtering power during deposition was 150 W. Further post-treatments of annealing (air furnace, 230°C for 30 min) and wet etching (1 wt.% NaOH aqueous solution at 40°C for 5 min) on the ZnO, AZO, and GZO films/glass were tested. The optical transmission properties of the films were recorded using a UV–VIS–NIR optical photometer (JASCO V570) with an integrating sphere (JASCO ISN-470) in the range of 300 to 1100 nm. The micro-morphology, surface roughness, and crystal properties of the films were determined by scanning electron microscopy (SEM, JEOL 6500), atomic force microscopy (AFM, NT-MDT Solver P47), and X-ray diffraction (XRD, PHILIPS X'Pert Pro).

II. Experimental Procedure

ZnO, AZO, and GZO thin films with thicknesses of 200nm and 400nm were deposited on glass by RF magnetron sputtering using 4-inch-diameter targets of ZnO, AZO (ZnO: Al_2O_3 =98:2 wt. %, and GZO (ZnO:Ga_2O_3 = 95:5 wt. %). The base pressure of the deposition chamber was kept at 2.5×10^{-6} torr and the working pressure at 2.5×10^{-3} torr by a rotation-type mechanical

Zue Chin Chang is with the Department of Mechanical Engineering, National Chin-Yi University of Technology, Taichung, Taiwan (phone: +886-4-23924505 ext 7188; fax: +886-42-393-0681; e-mail: chang@mail.ncut.edu.tw).

pump and a turbo pump, and the sputtering power during deposition was 150 W. Further post-treatments of annealing (air furnace, 230°C for 30min) and wet etching (1 wt.% NaOH aqueous solution at 40°C for 5min) on the ZnO, AZO, and GZO films/glass were tested.

III. Results and Discussion

Fig. 1 shows SEM images of ZnO, AZO and GZO films with a thickness of 200 nm after post treatment of 230℃ annealing for 30 min and etching in 1 wt.% NaOH aqueous solution for 5 min. The films display well-crystallized angular grains and smooth grains; Figs. 1 (a), (c), and (e) top-view images show ZnO, AZO and GZO films with sub-micron and nano grain sizes., AFM of a zone of 2 μm x 2μm revealed that the (b) ZnO film had roughness values of 4.43 nm (Ra) and 5.56 nm (Rms), (d) AZO film had surface roughness values of 2.32 nm (Ra) and 3.02 nm (Rms), and (f) GZO film had the smallest surface roughness values of 1.06 nm (Ra) and 1.45 nm (Rms). Like those in Figs. 1 (a), (c), and (e), have sub-micron and nano-sized grains. The 400 nm GZO film had void defects on the surface, in contrast to the smooth surface of the 200 nm GZO film. However, both the 200 nm and 400 nm films of ZnO and AZO had continuous, smooth surfaces.

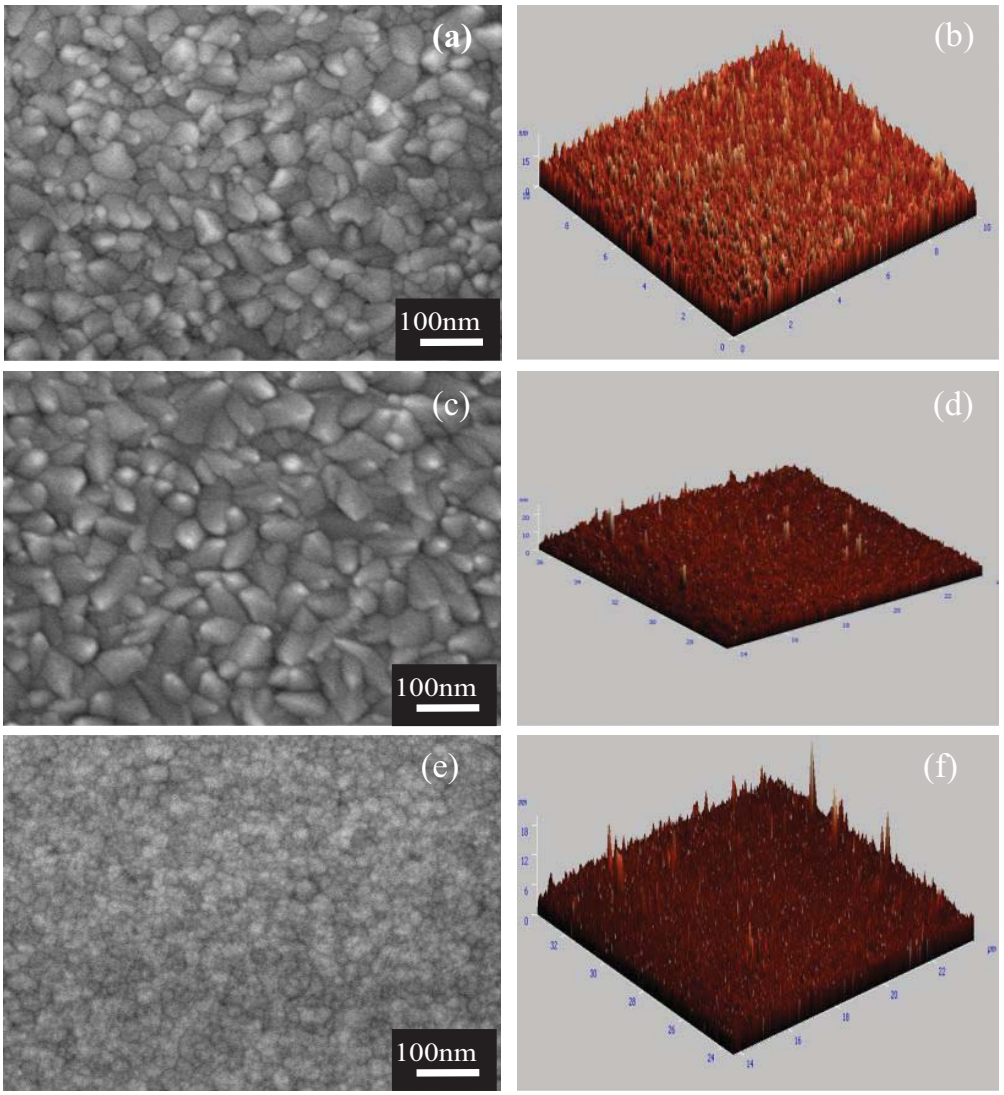

Fig. 1 SEM images of ZnO, AZO and GZO films after annealing at 230℃ for 30 min and etching in 1 wt.% NaOH for 5 min; (a), (c), and (e) top-view images show ZnO, AZO and GZO films with sub-micron and nano grain sizes., AFM of a zone of 2 μm x 2μm revealed that the (b) ZnO film had roughness values of 4.43 nm (Ra) and 5.56 nm (Rms), (d) AZO film had surface roughness values of 2.32 nm (Ra) and 3.02 nm (Rms), and (f) GZO film had the smallest surface roughness values of 1.06 nm (Ra) and 1.45 nm (Rms).

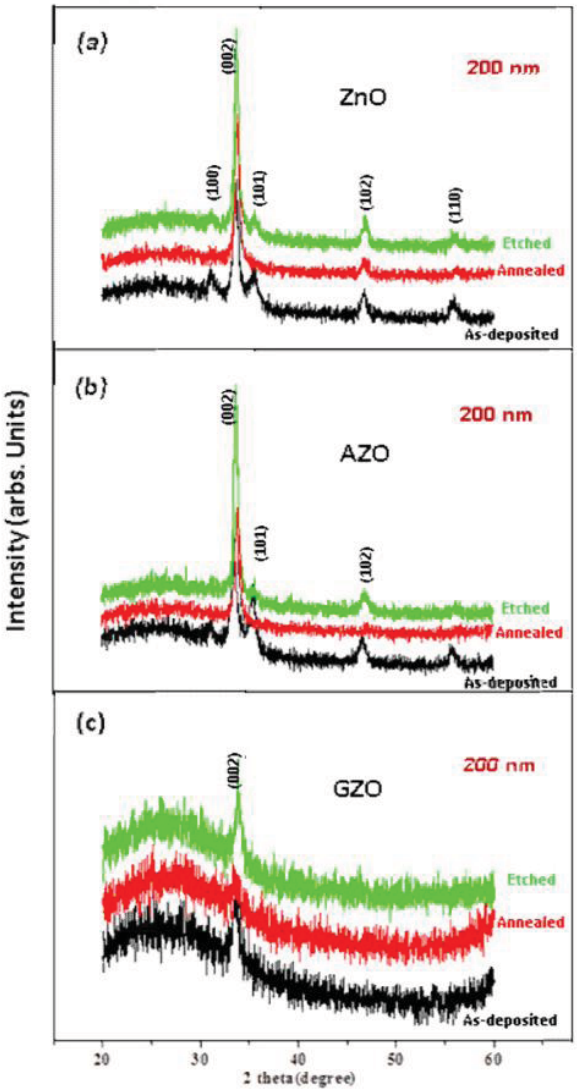

Fig. 2 XRD spectra of 200 nm films; (a) ZnO, (b) AZO, and (c) GZO films: as-deposited, annealed, and wet etched; the obvious grains presented after films were annealed and etched

Figs. 2 and 3 show the XRD spectra of the 200 nm and 400 nm ZnO, AZO, and GZO films. The deposited films were polycrystalline, with (100), (002), and (101) peaks of hexagonal ZnO at 31.75°, 34.35°, and 36.31°. The spectrum for dry aging indicated the presence of pure and polycrystalline ZnO in a wurtzite structure. However, the lower intensities of the spectrum peaks were magnified significantly by wet aging. Figs. 2 (b), (c), 3 (b), and (c) show XRD spectra of AZO and GZO films in different conditions. All films had a (002) preferred orientation. The crystallinity was weaker in the GZO film. In terms of the crystallization of the AZO film, the strong (002) and (101) peak orientations were apparent after wet aging, but this was not true for the GZO films. These orientations were due to the higher texture coefficient in the 1 wt.% NaOH alkaline environment of the AZO film. As for RF magnetron sputtering, in this case, the deposited films were found to feature mixed orientations in pure ZnO. Moreover, after wet aging of the AZO films, the c-axis (002) peak was sharply magnified, while the (101) peak was present but with much lower intensity and greater FWHM (full width at half maximum). In as-deposited ZnO, AZO, and GZO films, the orientation of the crystal growth may have been affected by the random atomic arrangement of the glass substrate. The nucleation of ZnO apparently occurred on the substrate interface, as indicated by the peak intensity of the (002) plane. Both dry aging and wet aging obviously changed the growth orientation of the grain surface, which may be readily triggered by the presence of slightly oriented grains, and hence the peak intensity of the (002) plane increased abruptly as aging progressed.

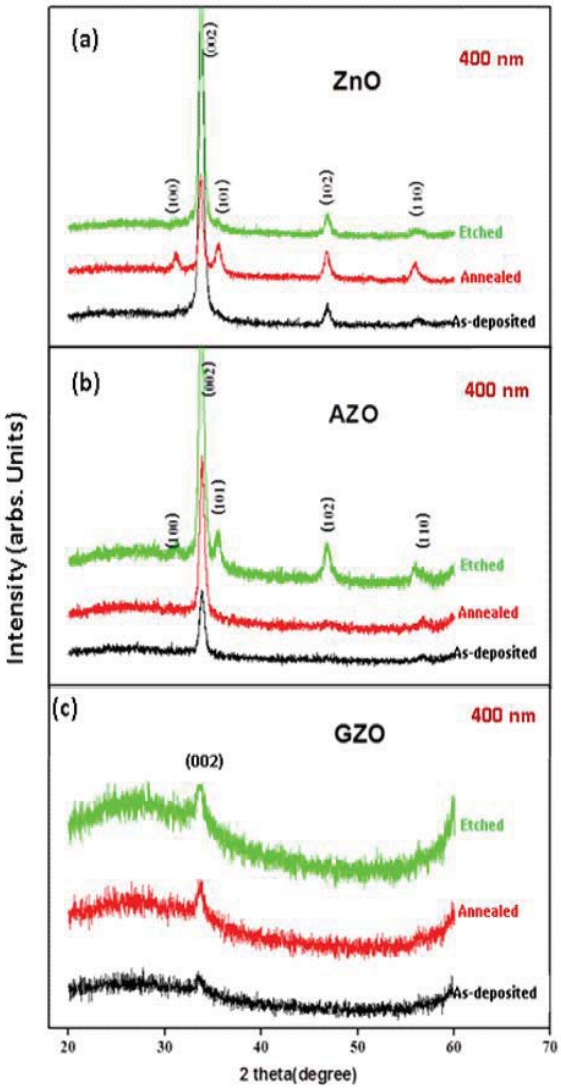

Fig. 3 XRD spectra of 400 nm films; (a) ZnO, (b) AZO, and (c) GZO films: as-deposited, annealed, and wet etched; the obvious grains presented after films were annealed and etched

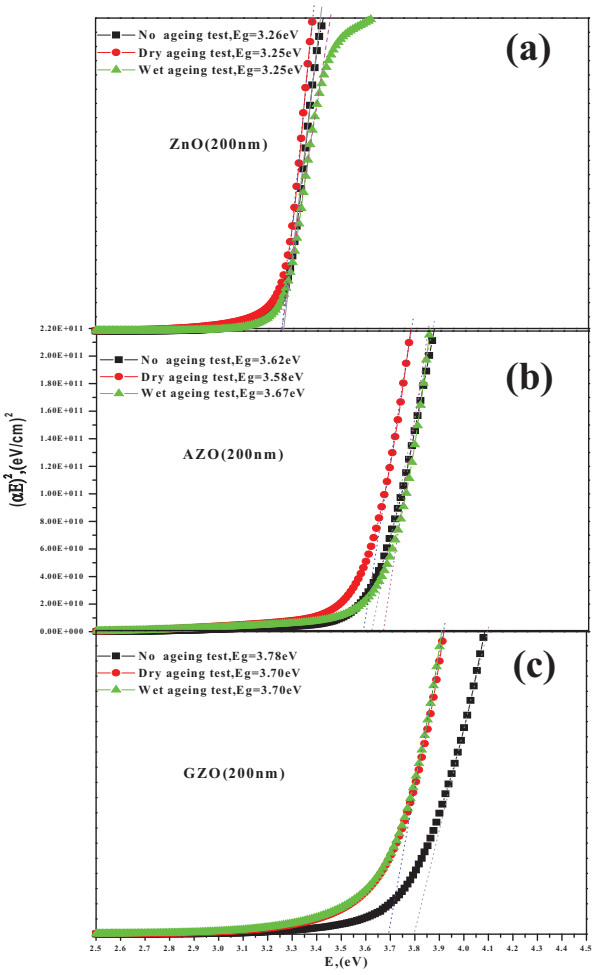

Fig. 4 Light absorption coefficient spectra of 200 nm films of ZnO, AZO, and GZO: (a) as-deposited, (b) annealed, and (c) wet-etched; the band gaps of annealed and etched films were stable as compared to the as-deposited films

Figs. 4 and 5 show furthermore computation results. We found that the optical band gaps of 200 nm thick as-deposited ZnO, AZO, and GZO thin films were 3.27, 3.62, and 3.78 eV. After dry-ageing test, the band gaps of the ZnO, AZO, and GZO thin films were 3.25, 3.58, and 3.70 eV, and after wet-ageing test, they were 3.25, 3.67, and 3.70 eV, respectively. The optical band gaps of 400 nm thick as-deposited ZnO, AZO, and GZO thin films were 3.28, 3.27, and 3.27 eV. After dry-ageing test, the band gaps of ZnO, AZO, GZO thin films were 3.49, 3.47, and 3.47 eV, and after wet-ageing test, they were 3.54, 3.53, and 3.53 eV, respectively. Thus, the differences in doping resulted in different gap values. According to the Burstein-Moss effect [17], highly doped n-type semiconductors will occupy the valence band at the bottom due to higher electronic concentration, broadening the band gap even further. The broadened optical energy gap increases the range of light penetration and therefore raises the penetration coefficient of short wavelength light. GZO film was found to have a larger penetration area of visible light and a larger band gap. ZnO, AZO, and GZO samples were annealed in the atmosphere as well as in an alkaline solution, and the optical properties of these samples are shown in Figs. 5 and 6. As a whole, the film penetration rate fell about 5% to 85%, owing greatly to film absorption, as shown by $T = \exp(-\alpha d)$ where T, α, and d represent transmission, absorption coefficient, and film thickness. Transmittance and the absorption coefficient were correlated in a negative natural logarithm under the same sample thickness. Light loss is basically caused by light being absorbed and diffused. It is noted that the absorption was obvious at 380 nm; thus, at wavelengths of 400-800 nm, the above causes can be ignored.

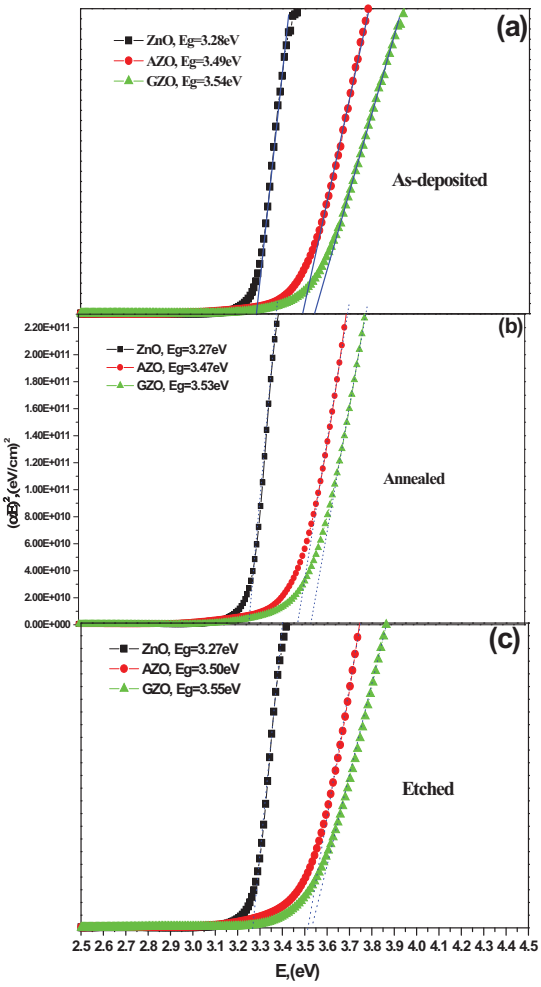

Fig. 5 Light absorption coefficient spectra of 400 nm films of ZnO, AZO, and GZO: (a) as-deposited, (b) annealed, and (c) wet-etched; the band gaps of annealed and etched films were stable as compared to the as-deposited films

Four causes of light diffusion have been proposed in the literature [18]: a) concentration of impurities, b) defects, c) surface roughness, and d) grain boundaries. Our analysis showed that the decline of light penetration was caused mainly by the concentration of impurities and grain boundaries. Under atmospheric annealing, the optical band gaps of the ZnO, AZO, and GZO thin films were 3.27~3.49, 3.47~3.58, and 3.47~3.70 eV. Theoretically, light transmission of shorter wavelengths should increase after annealing treatment. Aging treatment can increase the crystallinity of films, improving the transmittance rate of visible light, freeing electrons from defects, and reducing diffusion during electronic transmission. The carrier concentration is increased, moving towards the short wavelength range. In addition, oxygen in the air fills in the voids in the film during annealing, making the displacement less obvious. Under the alkaline environment, the optical band gaps of ZnO, AZO, and GZO thin films were 3.25~3.54, 3.53~3.67, and 3.53~3.70 eV, and the displacement of the gaps was obvious because the changes to the film were only superficial.

Fig. 6 and Table I show the four-point probe and Hall Effect measurements of the 400 nm thick ZnO, AZO, and GZO film assemblies under different aging treatments. The electric conduction mechanism of the AZO and GZO films came mainly from the Al and Ga, the oxygen vacancies, Zn interstitial atoms, and Al and/or Ga interstitial atoms. AZO and GZO films achieved higher conduction than did ZnO film, it being ion vacant and nonstoichiometric. AZO film had the lowest resistivity, lowest sheet resistance, and highest carrier concentration. The resistance of ZnO thin film was found to significantly increase as the annealing intensified. Tansley et al. [19] pointed out that the adsorbed oxygen ions (ionized absorbents) on the film surface can increase the energy barrier altitude and decrease the mobility and conductivity of the electrons. As a result, the oxygen absorbing electrons of ZnO thin film become oxygen deficient, and the flaw density and electronic density of the physical facilities were thus reduced. The chemical absorption of oxygen acted like an acceptor in the films, reducing the oxygen vacancies in the films and lowering the carrier concentration. Electronic resistivity was therefore greatly increased. The AZO and GZO thin films also had better anti-aging properties against the environment.

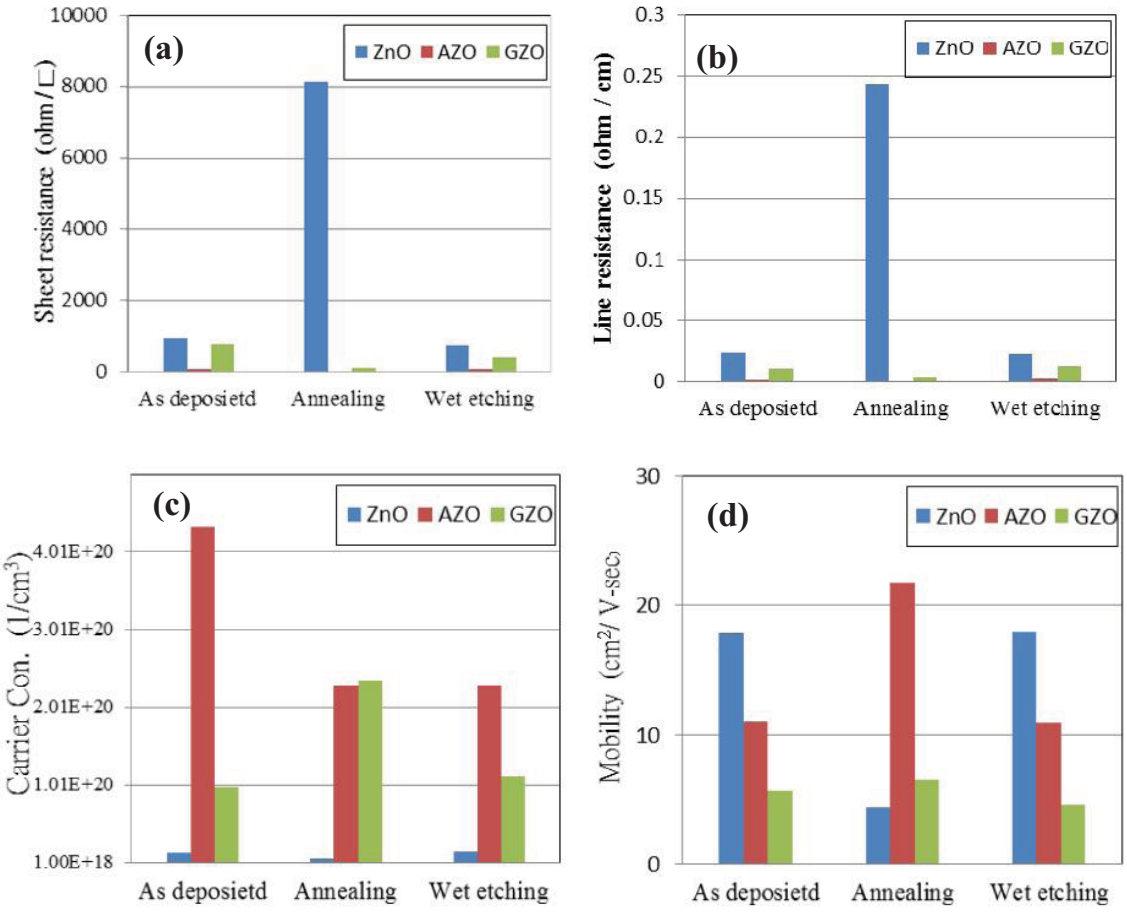

Fig. 6 The electrical properties of Zno, AZO, and GZO films; the AZO presented the best electrical properties

TABLE I
THE SHEET RESISTIVITY, LINE RESISTIVITY, CARRIER CONCENTRATION, AND MOBILITY CHARACTERIZATIONS OF ZNO, AZO, AND GZO FILMS WITH AS-DEPOSITED, ANNEALED, AND WET ETCHING TREATMENTS

Properties	ZnO			AZO			GZO		
	As-deposited	Dry Ageing test	Wet Ageing test	As-deposited	Dry Ageing test	Wet Ageing test	As-deposited	Dry Ageing test	Wet Ageing test
Sheet R (ohms per square)	958.5	8130.0	769.0	85.8	22.1	83.1	803.3	135.0	408.0
Resistivity$\times 10^{-3}$ (ohm-cm)	24.63	243.90	23.07	2.25	0.66	2.49	11.13	4.05	12.24
Carrier concentration$\times 10^{19}$(cm^{-3})	1.42	0.58	1.51	25.19	43.34	22.84	9.81	23.53	11.25
Mobility (cm^2/ V-sec)	17.90	4.40	17.95	11.03	21.72	10.96	5.71	6.55	4.53

IV. CONCLUSIONS

ZnO, AZO and GZO films were synthesized by RF magnetron sputtering. The above analytical results support the following conclusions.

1) Crystal columnar structures were observed in all the films. The AZO film was better crystallized, displaying angular grains. The voids in the GZO film made the continuity poor.
2) XRD analysis showed that all films exhibited the (002) preferred orientation. The spectrum for dry aging indicated the presence of pure and polycrystalline ZnO in a wurtzite crystal structure. However, the lower intensities of the spectrum peaks increased significantly during wet aging. In the crystallized AZO film, the strong (002) and (101) peak orientations were apparent after wet aging, but this was not the case for GZO films.
3) The penetration coefficient of those films reached about 90% at wavelengths of 400nm-800nm. We found that in the alkaline environment, the optical band gaps of ZnO, AZO, GZO thin films were 3.27, 3.47, and 3.53 eV. Both wet and dry aging treatments caused a decline of 5% in the average penetration rate due to increased impurities.
4) Hall measurements and four-point probe tests showed that the electrical properties of AZO and GZO films were better than those of ZnO film. Among them, AZO film presented the lowest resistivity, the best piece resistance, and the highest carrier density. The resistivity of ZnO film increased significantly with intensified air annealing. Both AZO and GZO films exhibited better anti-aging against the environment.

ACKNOWLEDGMENT

The authors gratefully acknowledge the financial support for this research by the National Science Council of Taiwan under grant no. NSC102-2622-E-167-001-CC3.

REFERENCES

[1] H. Kim, C. M. Gilmore, A. Pique, J. S. Horwitz, H. Mattoussi, H. Murata, Z. H. Kafafi, D. B. Chrisey, Electrical, Optical, and Structural Properties of Indium–Tin–Oxide Thin Films for Organic Light-Emitting Devices. J. Appl. Phys. 86 (1999) 6451-6461.
[2] Y. C. Lin, J. Y. Li, W. T. Yen, Applied Surface Science 254 (2008) 3262.
[3] H. M. Ali, M. M. Adb El-Raheem, N. M. Megahed, H. A. Mohamed, Journal of Physics and Chemistry of Solids 67 (2006) 1823.
[4] T. Minami, T. Miyata, Thin Solid Films, 517 (2008) 1474.
[5] H. J. Ko, Y. F. Chen, S. K. Hong, H. Wenisch, T. Yao, D. C. Look, Appl. Phys. Lett. 77 (2000) 3761.
[6] V. Assunção, E. Fortunato, A. Marques, H. Águas, I. Ferreira, M.E.V. Costa, R. Martins, Thin Solid Films, 427 (2003) 401.
[7] J. Ye, S. Gu, S. Zhu, T. Chen, L. Hu, F. Qin, R. Zhang, Y. Shi, Y. Zheng, Journal of Crystal Growth 243 (2002) 151.
[8] J. Zhao, L. Hu, W. Wang, W. Liu, A. Gong, Vacuum, 826 (2008) 664.
[9] S. H. Bae, S. Y. Lee, H. Y. Kim, S. Im, Opt. Mater., 17 (2001) 327.
[10] K. Sakurai, M. Kanehiro, K. Nakahara, T. Tanabe, S. Fujita, S. Fujita, Journal of Crystal Growth, 209(2000) 522.
[11] D. G. Baik, and S. M. Cho, Thin Solid Films, 354 (1999) 227.
[12] X. Yu, J. Ma, F. Ji, Y. Wang, X. Zhang, C. Cheng, H. Ma, Applied Surface Science, 239 (2005) 222.
[13] G. Gonçalves, E. Elangovan, P. Barquinha, L. Pereira, R. Martins, and E. Fortunato, Thin Solid Films, 515 (2007) 8562.
[14] T. Yamada, A. Miyake, H. Makino, N. Yamamoto, T. Yamamoto, Thin Solid Films, 517 (2009) 3134.
[15] W.T. Yen, Y.C. Lin, P.C. Yao, J.H. Ke, Y.L. Chen, Thin Solid Films, 518 (2010) 3882.
[16] F. Wu, L. Fang, Y.J. Pan, K. Zhou, H.B. Ruan, G.B. Liu, C.Y. Kong, Thin Solid Films, 520 (2011) 703.
[17] A. Sarkar, S. Ghosh, S. Chaudhury, A.K. Pal, Thin Solid Films 204 (1991) 255.
[18] P .Gao, L.J. Meng, M.P. dos Santos, V. Teixeira, M. Andritschky, Vacuum 56 (2000) 143.
[19] T. L. Tansley, D. F. Neely, Thin Solid Films, 121 (1984) 95.